Aerosol and Air Quality Research

ORIGINAL RESEARCH
https://doi.org/10.4209/aaqr.220069

Low Transmission of Coronavirus via Aerosols during Outdoor Running Races and Athletic Events

Michael Riediker *

Swiss Centre for Occupational and Environmental Health (SCOEH), Winterthur, Switzerland

ABSTRACT

Introduction: Outdoor contacts were reported to rarely result in transmission of the severe acute respiratory syndrome coronavirus 2 (SARS-CoV-2). Little is known, however, about the risk during popular outdoor running events. This study assessed the transfer of aerosols from infected runners to other race participants.

Methods: In the experimental part of the study, a group of dummies was pulled at different speeds over an athletics track and field circuit. Fine aerosols were produced with a fog machine, large aerosols with a pesticide sprayer releasing food colorant, with the size matching the two size modes of human expiratory aerosols. The experimentally determined transfer rates fed a Monte Carlo simulation of different race distances, starting sequences and block sizes. Runners were modeled using start and end times of SwissCityMarathon — Lucerne participants and a previously published distribution of virus emission strengths. The race distance was divided into 10-meter segments in which the transfer from the sources to collocated runners was calculated.

Results: The experiments showed that fog and spray transfer decreased with increasing distance from the source. Increased speed was associated with decreased fog but increased spray transfer. The simulations suggest that more runners received small amounts of virus by fog-transfer. However, critical virus-transfers defined as more than 100 virus copies happened mostly by spray. The estimated rate of people getting a potentially infectious dose was in most races well below the simulated prevalence rate of virus-emitting runners, mostly about five-fold smaller. Changing from block starts to individual starts further reduced the estimated transfer. Only an artificial group running 30 km in close distance at high speed brought the rate above parity.

Discussion: These findings suggest that outdoor running events are associated with a low risk for virus infection as long as runners are not trailing each other over very long distances.

Keywords: SARS-CoV-2, Spray, Fine aerosol, Running, Outdoor

Received: February 11, 2022
Revised: May 24, 2022
Accepted: May 25, 2022

* **Corresponding Author:**
michael.riediker@alumni.ethz.ch

Publisher:
Taiwan Association for Aerosol Research
ISSN: 1680-8584 print
ISSN: 2071-1409 online

1 INTRODUCTION

The severe acute respiratory syndrome coronavirus 2 emerged in late 2019 in Wuhan, China, and spread rapidly across the globe (Hsih *et al.*, 2020; Korean Society of Infectious Diseases *et al.*, 2020; Zhou *et al.*, 2020). The virus is easily transmissible between humans and was detected early in the air of hospitals (Liu *et al.*, 2020). Today, transmission by respiratory microdroplets is recognized as the predominant route of infection (Greenhalgh *et al.*, 2021; Morawska and Cao, 2020; Randall *et al.*, 2021; Zhang *et al.*, 2020). These respiratory droplets are formed during normal breathing, which produces mostly aerosols around 1 μm in diameter (Morawska *et al.*, 2009). More is released when people are talking and singing with a bimodal aerosol emission consisting of fine aerosols around 2 μm and larger aerosols between 20 and 200 μm (Asadi *et al.*, 2020, 2019; Hamner *et al.*, 2020; Johnson and Morawska, 2009). Similarly sized aerosols are also released during physical exercise (Wilson *et al.*, 2021).

There are considerable differences in transmission processes between indoor and outdoor settings. Indoors, virus-loaded fine aerosols can accumulate and rapidly create infectious concentrations if the infected person has a high viral load (Riediker and Tsai, 2020). While outdoors wind transport

of large droplets is of concern in the range of a few meters (Feng *et al.*, 2020), they are likely to disperse rapidly in the atmosphere. Another difference concerns the airborne half-life of the virus, which is in the range of over an hour when hovering in the dark (van Doremalen *et al.*, 2020) while it is reduced to a few minutes when exposed to simulated sunlight (Schuit *et al.*, 2020). Such differences translate into the transmission risk. Already early in the pandemic, outdoor settings were found to contribute little to the spread of the disease (Bulfone *et al.*, 2021; Leclerc *et al.*, 2020), estimated at well below 10% of all transmissions (Bulfone *et al.*, 2021). A more recent assessment of over 1.7 million PCR-confirmed cases in England used contact tracing data to link index cases and their contacts and attributed only 2.9% of all infections to outdoor contacts (Lee *et al.*, 2021). A review of airborne RNA measurements in indoor and outdoor settings also reported mostly undetectable quantities of viruses outdoors and much lower levels in crowded or close contact situations compared to similar indoor situations (Dinoi *et al.*, 2022).

Also in outdoor sports, virus transmission appears to be low. An analysis of the Danish football (soccer) league found no signs of transmission chains between the players. However, it was a cohort with a very low incidence rate (Pedersen *et al.*, 2021). Also, a study in professional golfers competing in 23 events during the PGA European Tour did not find any transmission, though it also had the limitation of a very low incidence rate (Robinson *et al.*, 2021b).

Running events represent a special type of outdoor contacts. In most situations, the participants of a race do not interact with each other, yet depending on their speed and starting schedule, they may spend prolonged time next to each other. Computational fluid dynamics models suggest that most large droplets emitted by a runner will drop rapidly in the slipstream but that some droplets may still reach a person trailing the source within 10 meters distance (Blocken *et al.*, 2020). An ongoing prospective study of Dutch runners assessed symptoms indicative of COVID-19 but did not find any association with running behavior and habits (Cloosterman *et al.*, 2021), suggesting that the risk of infection is likely low during outdoor trainings. More challenging is the situation for organizers of popular races. They need to consider (1) the risk of transmission from pre- and post-race activities and (2) the risk from running in large crowds. The first risk is common to many outdoor events and strategies established for such events can be followed (Honein *et al.*, 2020). This study aimed to evaluate the second risk, the one from running as a larger crowd. The proportion of aerosols transmitted to subsequent runners as a function of speed and distance was investigated; and the consequences of this transmission for the risk of infection of participants in races with different starting regimes were simulated.

2 METHODS

2.1 Study Design

The study was designed to collect experimental data under real-world conditions and to use the results for a subsequent simulation of different races and starting regimes. The experimental part assessed what proportion of the emitted aerosols gets transferred from a running person to those trailing at positions and distances similar to a race. The goal to assess the proportion relates to the fact that the virus number contained in a microdroplets is expected to remain stable during the short transfer time even if the microdroplets would shrink. To cover both modes of human aerosol emissions (fine aerosols around 2 μm and larger aerosols between 20 and 200 μm), a setup was chosen as follows: Two emitter dummies were built so that they released either fine aerosols created by a theatrical fog machine, or larger color droplets produced with a professional pesticide sprayer. The fog machine and the pesticide sprayer were chosen so that the released aerosol matches the two modes of the distribution of exhaled human aerosols (Johnson *et al.*, 2011). Both forms of aerosol production have a much larger emission strength than human aerosol formation. The high emission rates allowed ignoring the (low) background aerosol. For the fog, the number concentration of $PM_{2.5}$ was chosen because we had tested this type of aerosol experimentally and found that the $PM_{2.5}$ number concentration was stable for several minutes even in wind tunnels and very large halls. For the larger spray aerosols, a colorant was added to the liquid so that the transfer of the released aerosol could be determined. The amount of virus transferred was then calculated based on the documented emission size distribution (Johnson *et al.*, 2011) and the transfer rates determined during the experiments.

A group of seven runner dummies equipped with sensors was crafted and pulled behind one of the two emitters at a time at different speed over the 400 m athletics track and field circuit of the Deutweg sports grounds in Winterthur, Switzerland. Each experiment lasted one circle. The computational part of the study consisted of a Monte Carlo simulation of the dose received by runners from an infected participant during races of different length, starting sequence and starting block size. It used for this the proportion of fog and spray aerosols emitted by a source reaching trailing runners at different distance and speed.

2.2 Specification of the Measurement Dummies

Seven measurement dummies were crafted using 4 mm thick plywood. Each dummy had a torso of 595 mm height and 416 mm width. The dummy head was made of a bent polystyrene mirror and presented a cross-sectional surface of 250 mm × 146 mm. The head was made so that blotting paper could easily be mounted to later collect the sprayed aerosol. Behind each polystyrene mirror, an optical particle sensor was installed. The dummies were mounted on a structure attached to an e-bike's rack and on top of a cycle trailer. The height of the mounted dummies was 1720 mm, 1760 mm and 1680 mm at the source, the rack, and on the trailer, respectively. The dummies were arranged in three rows at a distance of about 1 (Position 1 and 2), 2 (Position 3 to 5) and 3 meters (Position 6 and 7) from the source. Fig. 1 shows the overall arrangement with the fog-head mounted as source. A detailed description with exact measures is provided in the Supplementary Material.

2.3 Measurement Devices

Fine aerosol counts in the $PM_{2.5}$ size range were measured at 1 Hz interval with a miniature optical particle counter (SPS30, Sensirion AG, Switzerland) that reports the numbers in four size bins (< 0.5 μm, < 1 μm, < 2.5 μm and < 10 μm). The Sensirion SPS30 sensor is a low-cost sensor that provides long-term stable measurements (Tryner *et al.*, 2020). The sizing, mass and number concentrations compare well to general ambient aerosol and also artificially created aerosols as long as the size of the aerosol is within the detection range of the sensors (Kuula *et al.*, 2020).

Fig. 1. Arrangement of the dummies, here shown with the fog-emitting source.

For the portion of the aerosol that is within the detectable size-range it provides a good between-sensor and repeat measurement accuracy (Hong *et al.*, 2021). Also at high humidity, the sensors perform well, which was the finding of a long-term assessment in Taiwan, a country with frequent high humidity conditions (Hong *et al.*, 2021). For the analysis of experiments, only the number concentration in the $PM_{2.5}$ size range was used. Before and after data acquisition, the sensors were cross-corrected using individual correction-factors for each sensor to obtain an accuracy of ±3% after correction.

Spray aerosol was collected onto extra white A3+ blotting paper (local stationery shop). The sheets of blotting paper were dried on site and stored in dry, dark conditions. All sheets were scanned at 300 dpi in TIFF-format (Epson WorkForce WF-7840, Seiko Epson Corp, Japan). The average color intensity across the entire sheet was analyzed with ImageJ (version 1.53a, National Institutes of Health, USA). The signal was first inverted, then the blue component of the RGB color spectrum was measured.

Calibration curves were obtained in separate spray experiments as follows: Humidity-adjusted blotting paper was weighted using a microbalance (EMB 2000-2, Kern & Sohn GmbH, Germany) before and immediately after varying amounts of food colorant mixture were sprayed onto the blotting paper. Spraying was done at room temperature and 85% relative humidity to avoid evaporative losses within the few seconds from spraying until weighing. Afterwards the paper was dried and stored in dry, dark conditions until optical analysis. The weight difference during calibration was highly and linearly correlated with the optical intensity measurements described above ($R^2 = 0.98$).

Before and after each running experiment, the spray container was weighted to obtain the amount of sprayed color. The amount of sprayed color deposited on the surface of a blotting paper was calculated from the measured color intensity and the calibration curve obtained in the laboratory calibration described above. The amount that would deposit on mouth, nose and eyes was assumed as 5% of what would deposit on the entire dummy head (1,825 mm^2 mouth, nose and eye, the cross-sectional surface of the dummy head was 36,500 mm^2).

The weather conditions on the days of the experiments were obtained from a weather station (WeatherScreen Pro, DNT Innovation GmbH, Germany) positioned on the track and field ground.

2.4 Generation of Aerosols

Theatrical fog was generated with a vaporizing fog generator (Power-Tiny, Look Solutions GmbH, Germany) that evaporates a mixture of tri-ethylene glycol, mono-propylene glycol, di-propylene glycol and demineralized water. When measuring with the mini-sensor used in the study, the emitted particles showed a mean diameter of ~1.5 μm. The emission strength of the fog machine was 5×10^{13} particles min^{-1} in the fine particulate matter ($PM_{2.5}$)-size range, determined with the mini-sensors in a wind-tunnel experiment (100,000 particles cm^{-3} after diluting the fog into 500 m^3 min^{-1}). To obtain the transfer rate for fine aerosols, the same size channel was used. The fog was conducted with a 32 mm wide tube to a hollow gypsum head on top of a torso and released through the mouth and nose openings at a steady flow.

The spray solution was created using a mixture of 79% w w^{-1} water, 19% w w^{-1} propylene glycol and 2% w w^{-1} red food colorant (E124 in propylene glycol, TRAWOSA AG, Switzerland). The spray was released through a hole at the mouth position of the face mirror of a dummy identical in build to the measurement dummies. The spray was guided through the mirror's surface 2 cm above the lower edge, spraying in the direction of travel. The spray was created with a professional grade pesticide sprayer with the pressure controlled at 3 bar and a 1.3 mm mist nozzle (Spraymatic 5S; constant pressure valve PR3; 1.3 mm Duro mist nozzle, all Birchmeier Sprühtechnik AG, Switzerland). This choice of spray pressure and nozzle was based on spray characterizations done by Birchmeier Sprühtechnik AG in partnership with the University of Lucerne using a phase Doppler anemometer (Dantec Dynamics, Denmark) on a measurement plane 60 mm in front of the nozzle with 225 (15 × 15) measurement points. Phase Doppler Anemometry assesses aerosols using the concept of doppler shift of laser light interacting with the flow field of moving aerosols (Durst *et al.*, 1997). The scattering angle between the emitting and receiving optics was 68°. The laser power in the measuring volume was about 9 mW. Fig. 2 shows the size distribution of the spray (Data kindly provided by Birchmeier Sprühtechnik AG). The spray was released as short bursts every two seconds.

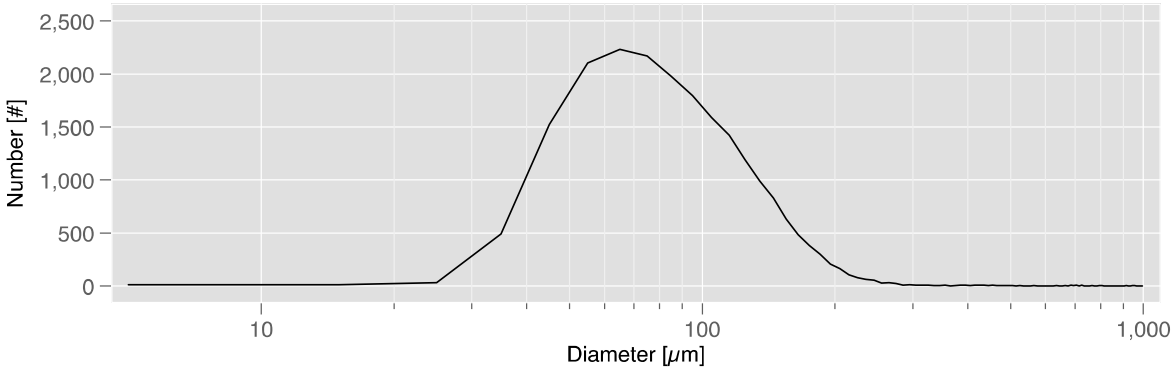

Fig. 2. Size distribution of the spray generated by the 1.3 mm mist nozzle at 3 bar pressure.

For each experiment, the spray emission was determined by gravimetrically assessing the weight of the spray system before and after the experiment.

5.5 Simulation and Statistical Analysis

All statistical analyses were done using STATA SE 15.1 (StataCorp, USA). The transfer between runners was simulated with a Monte Carlo approach. An overview graph describing the steps is shown in the Supplementary Material. First, a runner population was randomly drawn from an anonymized list of 9,647 participants of the SwissCityMarathon 2019 in Lucerne, Switzerland (kindly provided by the organizers) that contained the race time of all the participants over different distances. Then these runners were assigned starting times. Block starts were modeled so that twenty runners passed the start line every second in random order, independent of their later race performance. The same concept applied within each block of sequential block starts. Sequential individual starts were modeled with two seconds distance between runners.

For each runner participating in a simulated run, a random binomial draw decided first on the infection status of this runner based on the prevalence rate. Afterwards, the virus emission strength into the fog-size range of each of these positive runners was drawn from a previously modeled emission distribution of a population of people infected with a variant producing very high viral loads (distribution " O × 100" in Riediker *et al.*, 2022) and scaled to 100% speaking quietly at high physical activity, which corresponds to the emission part of the indoor scenario simulator (Riediker *et al.*, 2022; Riediker and Monn, 2021; Riediker and Tsai, 2020). For the spray emission, the virus emission strength was calculated on the basis of the number of viruses contained in the volume of an average emitted "large spray" droplet at the viral load of this emitter (Johnson *et al.*, 2011).

Within each 10-meter segment of the race, a pairwise comparison was done between runners. The virus transfer was calculated if a runner was collocated in that segment behind an emitter. For calculating the amount of virus transferred, experimental data was used for the combination of the nearest distance between the runners and the nearest speed of the rear runner as follows: For the fog, a random draw defined the fog transfer rate, combined with the above-described emission strength of that runner. For the spray, the number of droplets emitted in the time spent in the segment was calculated, followed by the determination of the number of droplets transferred to the trailing runner. This was determined with a binomial draw using the transfer rate as droplet impact probability. Experimental data is available only for the first three meters of a segment. Previous research suggests that emitted microdroplets from runners can reach runners trailing up to ten meters, while the slip-stream of a runner modulates the sedimentation and distribution of emitted microdroplets only in the first few meters (Blocken *et al.*, 2020). For runners farther than the last row ($>$ 3 m), transfer rates of the last row were assumed to linearly decrease down to zero until 10 meters distance. At the completion of a simulated race, the cumulative virus dose received via fog, spray and in total was calculated for each runner.

This random simulation of a race was repeated 1000 times for each studied race type. Afterwards, the proportion of runners receiving different doses during these races was calculated. In addition, for the 10 km race with a 100 person block start, different prevalence rates for starting infected runners were tested.

3 RESULTS AND DISCUSSION

3.1 Experimental Assessment of Transfer Rates

In total 29 experiments were conducted on 4 different days in July 2021, each consisting of a full round of 400 meters driven on the athletics track and field circuit. In total 18 rounds were with the fog source and 11 with the spray device; 11 rounds were at slow (10 km h^{-1}), 9 at medium (15 km h^{-1}) and 9 at fast (20 km h^{-1}) speed. On the days of the experiments, the weather situation varied from "sunny and hot" to "cloudy and windy with intermittent showers". To protect the equipment, no experiments were done while it was raining. During the experiments, temperature ranged from 18.0°C to 27.4°C (mean: 21.5°C, SD: 2.9°C), relative humidity from 37% to 74% (59.6%, 12.8%) and wind from 0 m s^{-1} to 3.4 m s^{-1} (1.2 m s^{-1}, 0.6 m s^{-1}).

Visually, the released fog flowed around the head to then rapidly become turbulent and well mixed across the runner field after the first row of runners. The two front runners were only partly in the fog stream. Fig. 3 shows a box plot of the number of fine aerosols measured in one-second intervals at the different positions and speed during all the tests conducted with theatrical fog. The optical sensors did not show any peaks nor any significant differences from background during the spray experiments. The concentrations were measured at occasionally high humidity levels. However, also at the highest level of 74% relative humidity, the uncertainties of the obtained values should remain in a reasonable range (Hagan and Kroll, 2020). A limitation is that the count values are above the coincidence levels of the sensors, which puts some doubts on the accuracy of the number concentrations. Fig. 3 clearly shows that the number concentration decreases with the dilution as the runners' speed increases. Furthermore, we found in wind tunnel experiments that the dilution factors are accurately described for the same test aerosol used in these runner experiments. This suggests that the sensors have a reasonably working algorithm to address coincidence, at least for the aerosol used in these experiments.

In the spray experiments, the exit jet of the nozzle was visible but the droplet trajectory could not be observed in the outdoor setting. However, the dummies' body and head became rapidly colored. Fig. 4 shows the proportion of spray deposited on the head on a surface equivalent to mouth, nose and eyes at different positions and speed during a full 400-meter round on the track and field circuit.

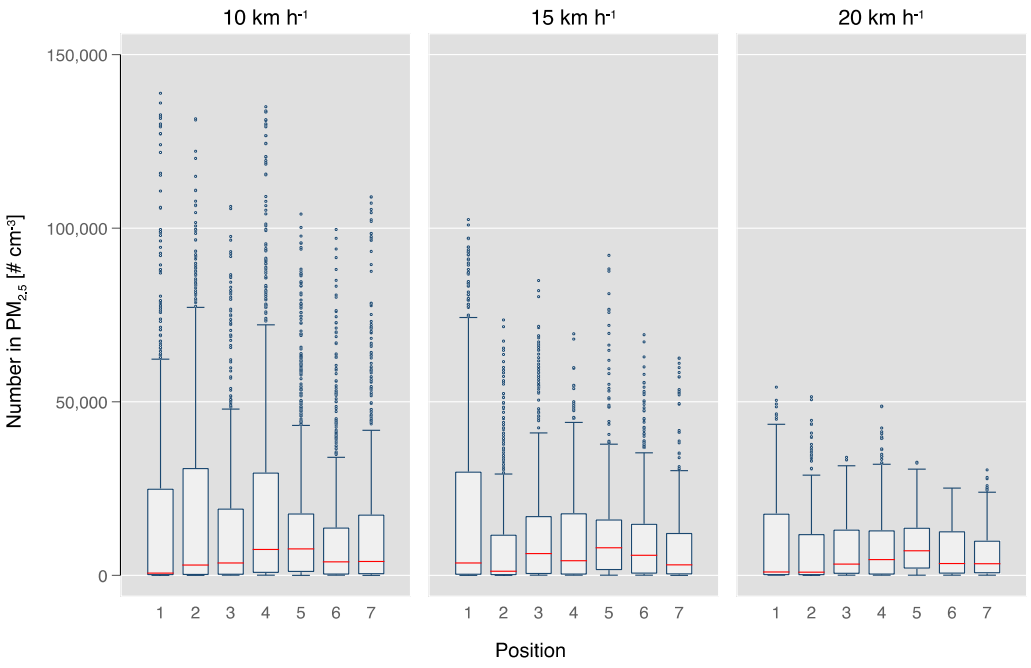

Fig. 3. Box plot of the number concentrations in the $PM_{2.5}$ size range measured at different positions and speed. Positions: 1 and 2: left and right in front row; 3, 4 and 5: left, middle and center of second row; 6 and 7: left and right of back row.

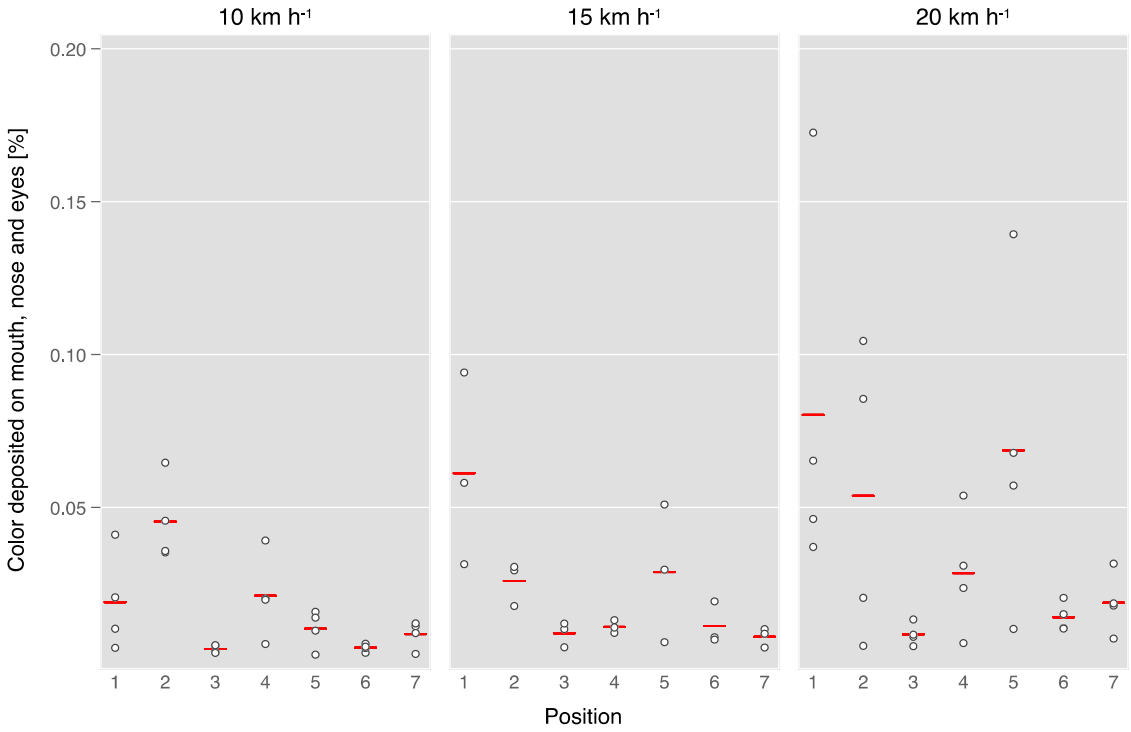

Fig. 4. Proportion of sprayed color deposited on the dummies' head on a surface equivalent to mouth, nose and eyes at different position and speed. The red line indicates the mean across all experiments, the dots the average of the individual circles on the 400 m athletics track. Positions: 1 and 2: left and right in front row; 3, 4 and 5: left, middle and center of second row; 6 and 7: left and right of back row.

The spray droplets showed large variability not only with distance but also in orthogonal direction. Regression analysis showed that the amount of deposited spray significantly increased with speed and decreased with distance. The pattern of the fog concentrations was complex. While the highest values were observed at Positions 1 and 2 (sidewards behind the source), these runners did not have the highest mean exposure, which can be attributed to the fog being channeled between them, as suggested by the visual observations. For the runners further back, the fog concentration significantly decreased with speed and distance.

Distance and speed of the runners influence the transfer rates, but also the flow field generated by the moving bodies especially very close behind the source, which is consistent with computational fluid dynamics simulations (Blocken *et al.*, 2020).

3.2 Findings of Monte Carlo Simulation

For the simulated race with 100 runners starting as a block, three different prevalence rates, 0.25%, 1% and 10% were used. Table 1 shows the summary statistics and the percentage of runners receiving a virus dose above 1, 10, 100, 1,000 and 3,000 virus copies, respectively. The mean received doses increased proportional to the prevalence rate. The fine aerosols, simulated in the experiments with the theatrical fog, contributed very little to the total dose. The maximal dose from fog suggests that for low prevalence rates, virus doses from fog will remain below 100 virus copies. An analysis of the timelines showed that fog exposure was frequent but at very low levels. Overall, fine aerosol seems to contribute relevant doses only when a very large proportion of runners is positive. In contrast, the maximal doses from spray were very high and not well related to the prevalence rate. An analysis of the timelines showed that most high doses can be traced back to only a few spray droplet transfer event. With increasing prevalence rates, a few runners were receiving spray droplets more than once during the race.

A more refined understanding can be gained when looking at the proportion of runners receiving doses above given values. The proportion of runners receiving very high doses above 3,000 virus copies is about ten-times smaller than the prevalence rate, while the proportion of

Table 1. Summary statistics and proportion of runners receiving different doses during a 10 km race with 100 participants who start all at the same time. The transmission was studied for different prevalence rates in a running population infected with Omicron. For each prevalence rate 1000 races were simulated.

	Prevalence rate (% infected)		
	0.25%	1%	10%
Summary statistics			
Mean fog dose (virus copies)	0.006	0.022	0.229
Maximum fog dose (virus copies)	55	79	298
Mean spray dose (virus copies)	3.69	28.5	150.4
Maximum spray dose (virus copies)	109'100	663'000	192'000
Proportion of runners receiving a dose ...			
... over 3,000 virus copies	0.022%	0.063%	0.602%
... over 1,000 virus copies	0.027%	0.090%	0.835%
... over 100 virus copies	0.044%	0.150%	1.302%
... over 10 virus copies	0.061%	0.207%	1.886%
... at least 1 virus copy	0.111%	0.481%	4.808%

those receiving at least one virus copy is about half the prevalence rate. For the critical dose of 100 virus copies, the proportion was four to seven times below the prevalence rate.

Table 2 summarizes the findings for the different types of races and starting regimes. For most simulated races, the proportion of runners receiving a potentially infectious virus dose was small. The race with 500 participants suggests that changing the starting procedure from a single block start to five smaller blocks of 100 participants leads to a clear reduction in potential virus transfer. Introducing single starts every two seconds further reduces this, as seen also for the race with 1,000 participants. Running a short athletics race of 1,500 meters in a group running on average at the same speed but with speed variations on each 10 meter segment also gave an infection risk below the prevalence rate. However, an exception among the simulations is the artificial situation of a 30 km race where runners are trailing each other in a fixed position over prolonged time, similar to a group of pacemakers. In this simulated group-race, having one positively tested participant resulted in several other runners likely getting an elevated dose.

Looking at the proportion of runners receiving doses above given values informs about the risk of infection. The infection risk starts to increase rapidly if the received dose is above the minimal infective dose. For the wild-type (the variant first described in Wuhan, China), we estimated this earlier to be in the range of 500 virus copies determined by the Polymerase Chain Reaction (PCR) method, for the Delta variant around 300 virus copies and for Omicron around 100 virus copies (Riediker *et al.*, 2022; Riediker and Monn, 2021). The Monte Carlo simulation of the races suggests the infection risk in popular running events to be low even in a pessimistic scenario that takes the critical dose as criterion for infection or not. This is consistent with the findings of low contributions

Table 2. Proportion of runners receiving different doses for different types of races at a prevalence rate of 0.25%. Each race type was simulated 1000 times.

Race type	Proportion (%) of runners receiving a virus dose...		
Distance, no. of runners, starting regime	... over 1000	... over 100	... over 10
10 km, 100 runners, all at same time	0.026%	0.042%	0.055%
10 km, 100 runners, 1 every 2 seconds	0.010%	0.015%	0.029%
10 km, 500 runners, all at same time	0.102%	0.160%	0.219%
10 km, 500 runners, 5 × 100 at same time	0.036%	0.058%	0.084%
10 km, 500 runners, 1 every 2 seconds	0.032%	0.045%	0.062%
10 km, 1000 runners, all at same time	0.146%	0.244%	0.337%
10 km, 1000 runners, 1 every 2 seconds	0.034%	0.058%	0.081%
1.5 km, 20 runners, variable 20 ± 2 km h^{-1}	0.045%	0.055%	0.055%
30 km, 11 runners, fixed formation	0.582%	0.755%	0.836%

of outdoor encounters to the spread of the disease (Lee *et al.*, 2021) and the absence of transmission chains in other types of outdoor sports (Pedersen *et al.*, 2021; Robinson *et al.*, 2021b) and running practices (Robinson *et al.*, 2021a).

4 CONCLUSIONS

The experiments suggest that only a small proportion of fine (fog) and larger (spray) respiratory aerosol gets transferred from a source to trailing runners. For popular races, a strategy to keep the runners' risk low is to switch from mass starts to individual starts. The simulations suggest that having every two seconds a single runner start reduces the risk by a factor of three to four compared to a mass start. The risk reduction achieved by this measure is much more pronounced for large races with many participants. However, it should be noted that the estimated risk to participants in a 1,000-person race with single start every two seconds was still higher than the risk of a block start during a small race of 100 runners. Thus, more sophisticated start regimes may be needed such as blocks of individual starts. An additional approach to reduce the risk is to reduce spray transfer by avoiding proximity with rules that ensure sufficient lateral distance. While testing should be a routine element of every race, the simulation of a group running closely together shows that for such race types it will be crucial to ensure with a good testing strategy that no runner is infectious. Taken together this study suggests that most types of outdoor running events contribute very little to the spread of the disease, assuming that the protection strategies before and after the race are correctly defined.

ACKNOWLEDGMENTS

This study was financially supported by the associations Swiss Runners and Swiss Athletics. The spraying device including the nozzle was kindly donated by Birchmeier Sprühtechnik AG, Switzerland. The city of Winterthur, Switzerland kindly gave access to the track and field circuit. A big thank you goes to all the athletes in Winterthur and the field-keeper for welcoming the pulk of dummies on their grounds.

SUPPLEMENTARY MATERIAL

Supplementary material for this article can be found in the online version at https://doi.org/10.4209/aaqr.220069

REFERENCES

Asadi, S., Wexler, A.S., Cappa, C.D., Barreda, S., Bouvier, N.M., Ristenpart, W.D. (2019). Aerosol emission and superemission during human speech increase with voice loudness. Sci. Rep. 9, 2348. https://doi.org/10.1038/s41598-019-38808-z

Asadi, S., Bouvier, N., Wexler, A.S., Ristenpart, W.D. (2020). The coronavirus pandemic and aerosols: Does COVID-19 transmit via expiratory particles? Aerosol Sci. Technol. 54, 635–638. https://doi.org/10.1080/02786826.2020.1749229

Blocken, B., Malizia, F., Van Druenen, T., Marchal, T. (2020). Towards aerodynamically equivalent COVID19 1.5 m social distancing for walking and running. White Paper. http://www.urbanphysics.net/Social%20Distancing%20v20_White_Paper.pdf (accessed 27 January 2022).

Bulfone, T.C., Malekinejad, M., Rutherford, G.W., Razani, N. (2021). Outdoor transmission of SARS-CoV-2 and other respiratory viruses: A systematic review. J. Infect. Dis. 223, 550–561. https://doi.org/10.1093/infdis/jiaa742

Cloosterman, K.L.A., van Middelkoop, M., Krastman, P., de Vos, R.J. (2021). Running behavior and symptoms of respiratory tract infection during the COVID-19 pandemic. J. Sci. Med. Sport 24, 332–337. https://doi.org/10.1016/j.jsams.2020.10.009

Dinoi, A., Feltracco, M., Chirizzi, D., Trabucco, S., Conte, M., Gregoris, E., Barbaro, E., La Bella, G., Ciccarese, G., Belosi, F., La Salandra, G., Gambaro, A., Contini, D. (2022). A review on

measurements of SARS-CoV-2 genetic material in air in outdoor and indoor environments: Implication for airborne transmission. Sci. Total Environ. 809, 151137. https://doi.org/10.1016/j.scitotenv.2021.151137

Durst, F., Brenn, G., Xu, T.H. (1997). A review of the development and characteristics of planar phase-Doppler anemometry. Meas. Sci. Technol. 8, 1203–1221. https://doi.org/10.1088/0957-0233/8/11/002

Feng, Y., Marchal, T., Sperry, T., Yi, H. (2020). Influence of wind and relative humidity on the social distancing effectiveness to prevent COVID-19 airborne transmission: A numerical study. J. Aerosol Sci. 147, 105585. https://doi.org/10.1016/j.jaerosci.2020.105585

Greenhalgh, T., Jimenez, J.L., Prather, K.A., Tufekci, Z., Fisman, D., Schooley, R. (2021). Ten scientific reasons in support of airborne transmission of SARS-CoV-2. Lancet 397, 1603–1605. https://doi.org/10.1016/S0140-6736(21)00869-2

Hagan, D.H., Kroll, J.H. (2020). Assessing the accuracy of low-cost optical particle sensors using a physics-based approach. Atmos. Meas. Tech. 13, 6343–6355. https://doi.org/10.5194/amt-13-6343-2020

Hamner, L., Dubbel, P., Capron, I., Ross, A., Jordan, A., Lee, J., Lynn, J., Ball, A., Narwal, S., Russell, S., Patrick, D., Leibrand, H. (2020). High SARS-CoV-2 attack rate following exposure at a choir practice — Skagit county, Washington, March 2020. MMWR Morb. Mortal. Wkly. Rep. 69, 606–610. https://doi.org/10.15585/mmwr.mm6919e6

Honein, M.A., Christie, A., Rose, D.A., Brooks, J.T., Meaney-Delman, D., Cohn, A., Sauber-Schatz, E.K., Walker, A., McDonald, L.C., Liburd, L.C., Hall, J.E., Fry, A.M., Hall, A.J., Gupta, N., Kuhnert, W.L., Yoon, P.W., Gundlapalli, A.V., Beach, M.J., Walke, H.T., CDC COVID-19 Response Team, *et al.* (2020). Summary of guidance for public health strategies to address high levels of community transmission of SARS-CoV-2 and related deaths, december 2020. MMWR Morb. Mortal. Wkly. Rep. 69, 1860–1867. https://doi.org/10.15585/mmwr.mm6949e2

Hong, G.H., Le, T.C., Tu, J.W., Wang, C., Chang, S.C., Yu, J.Y., Lin, G.Y., Aggarwal, S.G., Tsai, C.J. (2021). Long-term evaluation and calibration of three types of low-cost $PM_{2.5}$ sensors at different air quality monitoring stations. J. Aerosol Sci. 157, 105829. https://doi.org/10.1016/j.jaerosci.2021.105829

Hsih, W.H., Cheng, M.Y., Ho, M.W., Chou, C.H., Lin, P.C., Chi, C.Y., Liao, W.C., Chen, C.Y., Leong, L.Y., Tien, N., Lai, H.C., Lai, Y.C., Lu, M.C. (2020). Featuring COVID-19 cases via screening symptomatic patients with epidemiologic link during flu season in a medical center of central Taiwan. J. Microbiol. Immunol. Infect. S1684118220300682. https://doi.org/10.1016/j.jmii.2020.03.008

Johnson, G.R., Morawska, L. (2009). The mechanism of breath aerosol formation. J. Aerosol Med. Pulm. Drug Deliv. 22, 229–237. https://doi.org/10.1089/jamp.2008.0720

Johnson, G.R., Morawska, L., Ristovski, Z.D., Hargreaves, M., Mengersen, K., Chao, C.Y.H., Wan, M.P., Li, Y., Xie, X., Katoshevski, D., Corbett, S. (2011). Modality of human expired aerosol size distributions. J. Aerosol Sci. 42, 839–851. https://doi.org/10.1016/j.jaerosci.2011.07.009

Korean Society of Infectious Diseases, Korean Society of Pediatric Infectious Diseases, Korean Society of Epidemiology, Korean Society for Antimicrobial Therapy, Korean Society for Healthcare-associated Infection Control and Prevention, Korea Centers for Disease Control and Prevention (2020). Report on the epidemiological features of coronavirus disease 2019 (COVID-19) outbreak in the Republic of Korea from January 19 to March 2, 2020. J. Korean Med. Sci. 35, e112. https://doi.org/10.3346/jkms.2020.35.e112

Kuula, J., Mäkelä, T., Aurela, M., Teinilä, K., Varjonen, S., González, Ó., Timonen, H. (2020). Laboratory evaluation of particle-size selectivity of optical low-cost particulate matter sensors. Atmosp. Meas. Tech. 13, 2413–2423. https://doi.org/10.5194/amt-13-2413-2020

Leclerc, Q.J., Fuller, N.M., Knight, L.E., CMMID COVID-19 Working Group, Funk, S., Knight, G.M. (2020). What settings have been linked to SARS-CoV-2 transmission clusters? Wellcome Open Res. 5, 83. https://doi.org/10.12688/wellcomeopenres.15889.2

Lee, L.Y.W., Rozmanowski, S., Pang, M., Charlett, A., Anderson, C., Hughes, G.J., Barnard, M., Peto, L., Vipond, R., Sienkiewicz, A., Hopkins, S., Bell, J., Crook, D.W., Gent, N., Walker, A.S., Peto, T.E.A., Eyre, D.W. (2021). SARS-CoV-2 infectivity by viral load, S gene variants and demographic factors and the utility of lateral flow devices to prevent transmission. Clin. Infect. Dis. ciab421. https://doi.org/10.1093/cid/ciab421

Liu, Yuan, Ning, Z., Chen, Y., Guo, M., Liu, Yingle, Gali, N.K., Sun, L., Duan, Y., Cai, J., Westerdahl, D., Liu, X., Xu, K., Ho, K., Kan, H., Fu, Q., Lan, K. (2020). Aerodynamic analysis of SARS-CoV-2 in two Wuhan hospitals. Nature 582, 557–560. https://doi.org/10.1038/s41586-020-2271-3

Morawska, L., Johnson, G.R., Ristovski, Z.D., Hargreaves, M., Mengersen, K., Corbett, S., Chao, C.Y.H., Li, Y., Katoshevski, D. (2009). Size distribution and sites of origin of droplets expelled from the human respiratory tract during expiratory activities. J. Aerosol Sci. 40, 256–269. https://doi.org/10.1016/j.jaerosci.2008.11.002

Morawska, L., Cao, J. (2020). Airborne transmission of SARS-CoV-2: The world should face the reality. Environ. Int. 139, 105730. https://doi.org/10.1016/j.envint.2020.105730

Pedersen, L., Lindberg, J., Lind, R.R., Rasmusen, H. (2021). Reopening elite sport during the COVID-19 pandemic: Experiences from a controlled return to elite football in Denmark. Scand. J. Med. Sci. Sports 31, 936–939. https://doi.org/10.1111/sms.13915

Randall, K., Ewing, E.T., Marr, L.C., Jimenez, J.L., Bourouiba, L. (2021). How did we get here: what are droplets and aerosols and how far do they go? A historical perspective on the transmission of respiratory infectious diseases. Interface Focus 11, 20210049. https://doi.org/10.1098/rsfs.2021.0049

Riediker, M., Tsai, D.H. (2020). Estimation of viral aerosol emissions from simulated individuals with asymptomatic to moderate coronavirus disease 2019. JAMA Netw. Open 3, e2013807. https://doi.org/10.1001/jamanetworkopen.2020.13807

Riediker, M., Monn, C. (2021). Simulation of SARS-CoV-2 aerosol emissions in the infected population and resulting airborne exposures in different indoor scena rios. Aerosol Air Qual. Res. 21, 200531. https://doi.org/10.4209/aaqr.2020.08.0531

Riediker, M., Briceno-Ayala, L., Ichihara, G., Albani, D., Poffet, D., Tsai, D.-H., Iff, S., Monn, C. (2022). Higher viral load and infectivity increase risk of aerosol transmission for Delta and Omicron variants of SARS-CoV-2. Swiss Med. Wkly. 152, 1–5. https://doi.org/10.4414/SMW.2022.w30133

Robinson, J.N., Fontana, M.A., Metzl, J.D., Dixit, S., Kliethermes, S.A., Quijano, B., Toresdahl, B. (2021a). Running races during the COVID-19 pandemic: a 2020 survey of the running community. BMJ Open Sport Exerc. Med. 7, e001192. https://doi.org/10.1136/bmjsem-2021-001192

Robinson, P.G., Murray, A., Close, G., Kinane, D.F. (2021b). Assessing the risk of SARS-CoV-2 transmission in international professional golf. BMJ Open Sport Exerc. Med. 7, e001109. https://doi.org/10.1136/bmjsem-2021-001109

Schuit, M., Ratnesar-Shumate, S., Yolitz, J., Williams, G., Weaver, W., Green, B., Miller, D., Krause, M., Beck, K., Wood, S., Holland, B., Bohannon, J., Freeburger, D., Hooper, I., Biryukov, J., Altamura, L.A., Wahl, V., Hevey, M., Dabisch, P. (2020). Airborne SARS-CoV-2 Is rapidly inactivated by simulated sunlight. J. Infect. Dis. 222, 564–571. https://doi.org/10.1093/infdis/jiaa334

Tryner, J., Mehaffy, J., Miller-Lionberg, D., Volckens, J. (2020). Effects of aerosol type and simulated aging on performance of low-cost PM sensors. J. Aerosol Sci. 150, 105654. https://doi.org/10.1016/j.jaerosci.2020.105654

van Doremalen, N., Bushmaker, T., Morris, D.H., Holbrook, M.G., Gamble, A., Williamson, B.N., Tamin, A., Harcourt, J.L., Thornburg, N.J., Gerber, S.I., Lloyd-Smith, J.O., de Wit, E., Munster, V.J. (2020). Aerosol and surface stability of SARS-CoV-2 as compared with SARS-CoV-1. N. Engl. J. Med. 382, 1564–1567. https://doi.org/10.1056/NEJMc2004973

Wilson, N.M., Marks, G.B., Eckhardt, A., Clarke, A.M., Young, F.P., Garden, F.L., Stewart, W., Cook, T.M., Tovey, E.R. (2021). The effect of respiratory activity, non-invasive respiratory support and facemasks on aerosol generation and its relevance to COVID-19. Anaesthesia 76, 1465–1474. https://doi.org/10.1111/anae.15475

Zhang, R., Li, Y., Zhang, A.L., Wang, Y., Molina, M.J. (2020). Identifying airborne transmission as the dominant route for the spread of COVID-19. Proc. Natl. Acad. Sci. 117, 14857–14863. https://doi.org/10.1073/pnas.2009637117

Zhou, F., Yu, T., Du, R., Fan, G., Liu, Y., Liu, Z., Xiang, J., Wang, Y., Song, B., Gu, X., Guan, L., Wei, Y., Li, H., Wu, X., Xu, J., Tu, S., Zhang, Y., Chen, H., Cao, B. (2020). Clinical course and risk factors for mortality of adult inpatients with COVID-19 in Wuhan, China: A retrospective cohort study. Lancet 395, 1054–1062. https://doi.org/10.1016/S0140-6736(20)30566-3